Available online at www.sciencedirect.com
SCIENCE DIRECT®
ELSEVIER
Journal of Catalysis 223 (2004) 241–249
JOURNAL OF CATALYSIS
www.elsevier.com/locate/jcat

1-Pentene epoxidation in catalytic microfabricated reactors

Yu Shan Susanna Wan,[a] Joseph Lik Hang Chau,[b] King Lun Yeung,[b] and Asterios Gavriilidis[a,*]

[a] *Department of Chemical Engineering, University College, London, Torrington Place, London WC1E 7JE, UK*
[b] *Department of Chemical Engineering, the Hong Kong University of Science and Technology, Clear Water Bay, Kowloon, Hong Kong, People's Republic of China*

Received 14 July 2003; revised 7 November 2003; accepted 10 November 2003

Abstract

Silicon-glass microreactors with TS-1 catalyst wall coatings were fabricated and used for 1-pentene epoxidation with hydrogen peroxide in continuous flow. Seeding of the microchannels before zeolite growth was necessary to obtain a small crystal size and a sufficient zeolite film thickness. Crystal size was further reduced by adjusting synthesis conditions and utilizing triethoxymethylsilane (TEMS) as a crystal growth inhibitor. Zeolite film morphology and crystal orientation did not show any significant effect on reactor performance. However, reaction rate was found to increase with decreasing TS-1 crystal size in the zeolite films and with increasing amount of tetrahedrally coordinated Ti(IV). Catalyst deactivation was observed, caused by the presence of organic compounds and Ti leaching from the microporous framework.

Keywords: Microreactor; Zeolite; Epoxidation; 1-Pentene; Titanium silicalite-1; Deactivation; Ti leaching

1. Introduction

There is a growing interest in the use of zeolite and molecular sieve materials as active components of miniaturized chemical systems such as chemical sensors, microreactors, microseparators, and Lab-on-a-Chip devices. Zeolite catalysts have been employed in microreactors for catalytic reduction of NO with ammonia [1], alkene epoxidation [2], and Knoevenagel condensation of benzaldehyde and ethyl cyanoacetate [3]. Zeolite micromembranes exhibit excellent permselectivity for gases and hydrocarbon vapors [4]. They also display good proton flux while selectively rejecting methanol, making them an attractive material for the construction of a miniature direct methanol fuel cell device (μ-DMFC) [5]. Robertson [6] described the use of zeolite adsorbents in a miniature column for gas separation.

Catalyst incorporation is a critical issue in microreactor fabrication. Sputter coating, thermal deposition, and chemical vapor deposition are some of the methods that can be used for deposition of catalysts in microreactors [7,8]. Metal oxide supports can be formed from the substrate by anodization [9,10], while powder catalysts can be packed in microchannels [11]. Although microfixed bed reactors are relatively easy to fabricate, they can exhibit a large pressure drop. Catalyst powders coated onto a smooth channel wall can delaminate during reaction, resulting in loss of activity and in some cases the detached powder can clog the microchannel.

Zeolites can be deposited and grown on silicon and glass substrates by hydrothermal synthesis. Jansen and van Rosmalen [12] were among the first to describe the growth of continuous zeolite film on a silicon wafer. Schoeman et al. [13] reported an improved method for synthesis of ultrathin silicalite-1 (Sil-1) film on silicon wafer. Den Exter et al. [14] prepared freestanding silicalite-1 membranes from deposited Sil-1 film by selective etching of the silicon substrate. Silicalite-1 films of different orientations and surface morphologies can be grown on silicon by controlled seeding [15,16]. This method affords a convenient way for manipulating the deposited zeolite film microstructure. Several strategies for incorporating zeolites within the design architecture of microreactors and microseparators have been described by Yeung and co-workers [4,17–19].

Titanium silicalite-1 (TS-1) prepared by isomorphous substitution of titanium ions into the MFI zeolite framework is an excellent selective oxidation catalyst [20–22]. TS-1 can catalyze many reactions including the conversion of alkenes to epoxides [23–25], alcohols to aldehydes [26], alkanes to secondary alcohols and ketones [27],

---

[*] Corresponding author.
E-mail address: a.gavriilidis@ucl.ac.uk (A. Gavriilidis).

0021-9517/$ – see front matter © 2003 Elsevier Inc. All rights reserved.
doi:10.1016/j.jcat.2003.11.001

phenol to hydroquinone and catechol [28], and amines to hydroxylamines [29] using hydrogen peroxide under mild conditions. These catalyzed processes are environmentally friendly and are characterized by their excellent product yield and selectivity. The aqueous hydrogen peroxide oxidant is transformed into water during the conversion. TS-1 has been employed in industrial processes like phenol hydroxylation and cyclohexanone ammoximation [30–33]. The later is an important industrial process for caprolactam production, the monomer of Nylon 6 [34].

In this work, a study of a titanium silicalite-1 microreactor for 1-pentene epoxidation is presented. A novel procedure for the fabrication of a TS-1 microreactor is described where the TS-1 catalyst is confined within the microchannel. The influence of zeolite structure and composition is studied by varying the synthesis conditions. Catalyst reactivity is investigated over time to examine catalyst deactivation.

2. Experimental

2.1. *Microreactor fabrication and zeolite catalyst incorporation*

The microchannel reactor was fabricated by patterning an LPCVD silicon nitride-coated Si(100) wafer, followed by etching with 30 wt% KOH at 80 °C for 6 h. The trapezoidal cross-sectional channel was 33 mm long, 500 µm wide at the top, and 220–250 µm deep. A layer of TS-1 zeolite catalyst was grown on the microchannel walls using the synthesis procedure described by Wan et al. [2]. Zeolite growth was confined within the walls of the microchannel by selective seeding with TS-1 zeolite nanocrystals. This was accomplished by first grafting mercapto-3-propyltrimethoxysilane onto the freshly etched microchannel. A colloidal suspension of zeolite nanocrystals was then added, depositing a layer of seeds onto the functionalized surface of the microchannel. The seeded sample was dried in oven at 333 K overnight, before calcining in air at 823 K for 6 h.

The colloidal TS-1 seeds were crystallized from a clear synthesis solution containing mole ratios of 20 tetraethyl orthosilicate (TEOS):0.75 tetraethyl orthotitanate (TEOT): 9 tetrapropylammonium hydroxide (TPAOH):404 H_2O at 398 K for 50 h. The zeolite seeds were recovered by a series of washing and separation steps and diluted with absolute ethanol to obtain a stable, 2 wt% colloidal suspension. X-ray diffraction confirmed that the seeds were MFI-type, TS-1 zeolite. An average particle size of 100 nm was determined by scanning electron microscope (SEM, JEOL JSM 6300) (see Fig. 1a). Chemical analyses by X-ray photoelectron spectroscopy (XPS, Physical Electronics PHI 5600), energy dispersive X-ray spectroscopy (EDXS, Oxford Instruments), and micro-Raman (Renishaw 3000) indicated that the colloidal TS-1 has a spatially uniform Si/Ti content of 20, with most of the titanium atoms incorporated within the zeolite framework. A BET surface area (Coulter, SA3100) of 425 m^2/g was measured for the calcined zeolite seeds.

The calcination step removed the organic template molecule (TPA^+) from the deposited TS-1 seeds. It also sintered the seeds into a stable layer and improved their adhesion on the channel wall. A layer of TS-1 catalyst was grown onto the seeded channel from a hydrothermal synthesis solution containing silicon and titanium precursors, as well as the TPA^+ organic template. The synthesis composition was adjusted to control the microstructure and titanium content of the catalyst layer. Triethoxymethylsilane (TEMS) was added to provide independent control over the zeolite grain size and

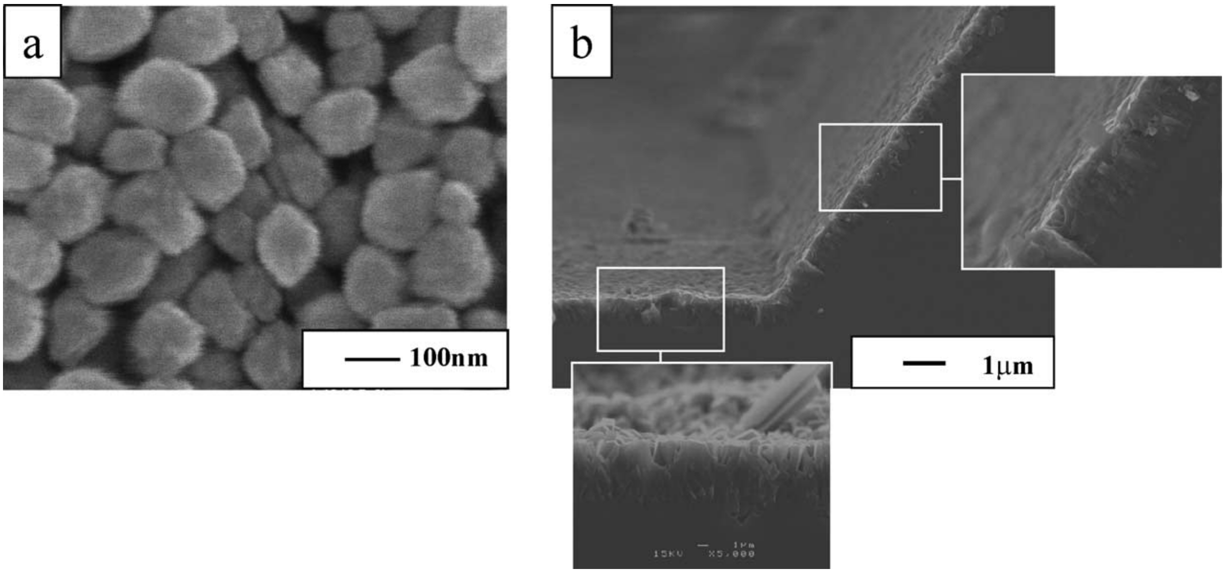

Fig. 1. Scanning electron microscope pictures of (a) TS-1 zeolite seeds and (b) TS-1 zeolite grown in a microreactor channel. (Note: inserts are twice the magnification of the picture.)

intergrowth. The sample was placed horizontally in a Teflon holder with the seeded microchannel facing downward. This was to prevent precipitates from the synthesis solution being deposited onto the growing zeolite layer. The sample and the solution were placed in a Teflon vessel and sealed within a stainless-steel autoclave. The synthesis was conducted in an oven at 448 K for 24 h. The TS-1 catalyst was calcined in air at 823 K for 24 h to remove the organic template molecules from the zeolite coating.

The microchannel reactor was inspected by optical microscope (Olympus BH-2) after each fabrication step. The dimensions of the microchannel (i.e., width and depth), the uniformity and precision of the zeolite incorporation, and the thickness and microstructure of the catalyst layer were determined by SEM. The structure, crystallinity, and orientation of the deposited zeolites were analyzed by X-ray diffraction (XRD, Philips W 1030). The titanium content was examined by XPS before and after reaction. A clean Pyrex glass cover was bonded onto the zeolite microreactor to complete the reactor assembly. A positive resist (SU-8) was coated onto the glass cover to serve as an adhesion layer. A leak-free seal was obtained after UV exposure. Tests showed that the sealing was able to withstand hydrocarbon solvents (i.e., methanol, MTBE, and 1-pentene) and reaction temperatures of up to 373 K. Predrilled holes on the glass cover served as inlets and outlets for the reactants and products.

2.2. 1-Pentene epoxidation

The microreactor experiments were conducted using a reaction mixture containing 0.9 M 1-pentene and 0.2 M hydrogen peroxide in methanol/water (volume ratio 50/1). The reaction temperature was kept at 298 K by a temperature-controlled water bath. A syringe pump (kdScientific) delivered the reactants with a flow rate of 100 µl/h. The product mixture was collected from the outlet, using sample vials cooled in acetone ice. One microliter of the reaction effluent was injected in a gas chromatograph (HP 6890) equipped with a Poraplot Q column (30 m, Chrompack) and a flame ionization detector. Three measurements were made for each sample and the concentrations of the reactants and products were determined using a calibration curve prepared from standard solutions containing known quantities of reactant (1-pentene), product (1,2-epoxypentane), and internal standard (*tert*-butyl methyl ether, MTBE).

Catalyst deactivation was investigated by measuring epoxypentane yield as a function of time. A reactor coated with 5-µm-thick, TS-1 zeolite film (initial Si/Ti = 30, crystal size 2–4 µm) was selected for the study. Analysis of the catalyst at various intervals was conducted using XPS, thermogravimetric, and differential thermal analyses (TGA/DTA, Setaram 92-18) to determine the possible causes of deactivation. Catalyst reactivation was conducted at 823 K in air for 24 h.

2.3. Materials

Chemicals used for zeolite synthesis included TEOS (98%, Aldrich), TEOT (95%, Merck-Schuchardt), TPAOH (1 M, Aldrich), and TEMS (99%, Aldrich). Mercapto-3-propyltrimethoxysilane (99%) employed for seeding was from Aldrich Chemicals. The Teflon holder and container were cleaned with 1 M nitric acid (BDH) solution under hydrothermal conditions at 423 K overnight to remove deposited zeolites. The 1-pentene (99%), hydrogen peroxide (30 wt%), MTBE (99.8%), and methanol (99.8%) used in the reaction experiments were from Fluka and BDH.

3. Results and discussion

3.1. Zeolite microreactor

A cross section of the microchannel (Fig. 1b) shows the TS-1 layer (2 at.% Ti) deposited on the microchannel wall. Zeolite growth was absent outside the seeded microchannel. The zeolite was uniformly deposited along the channel walls, forming a ca. 5-µm-thick film made up of intergrown 3-µm zeolite crystal grains (Fig. 1b, insets). The zeolite film displayed excellent adhesion to the channel and was able to withstand high-temperature treatments (823 K) without forming cracks or delaminating from the silicon substrate. Several TS-1 microreactors were prepared and tested in this study. Among the variables investigated were Ti content of the catalyst (0.9–3.5 at.%), zeolite film morphology and orientation (i.e., (101) and (020/200) orientations), and average zeolite crystal size (2–4.5 µm).

3.2. Effect of titanium incorporation and loading

Titanium silicalite-1 is an efficient catalyst for the epoxidation of alkenes to epoxides [23], allyl chloride to epichlorohydrin [35], allyl alcohol to glycidol [36], styrene to phenylacetaldehyde [37], and propylene to propylene oxide [38]. Diffusion of molecules through the narrow zeolite pore channel (0.55 nm) toward the active site can be a rate-limiting process in these reactions. Branched and cyclic alkenes tend to react more slowly than straight chain alkenes [23]. 1-Pentene epoxidation was chosen for its fast reaction rate. The reaction between 1-pentene and hydrogen peroxide over TS-1 catalyst produces 1,2-epoxypentane. The principal by-products are glycols and glycol monoethylethers [23].

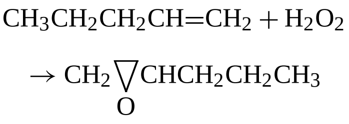

$$CH_3CH_2CH_2CH{=}CH_2 + H_2O_2 \rightarrow CH_2\underset{O}{\bigtriangledown}CHCH_2CH_2CH_3$$

Reaction tests conducted on bare silicon, TiO_2-coated (P25, Degussa), and anatase TiO_2-coated (Hombikat UV100, Sachtleben) microreactors showed that these materials are inactive for 1-pentene epoxidation. Experiments indicated that the structurally identical silicalite-1 (Sil-1) zeolite was also inactive for the reaction.

Synthesis of TS-1 zeolite is difficult to control and can result in poor reproducibility [20]. Even under optimal synthesis conditions, the titanium content of the zeolite samples can vary significantly leading to a large difference in their catalytic activity. The insertion of titanium atoms in the zeolite framework is strongly affected by the chemical nature of the titanium and silica precursors, solution pH, and synthesis temperature [39]. The typical TS-1 synthesis composition from the literature (30 TEOS:1.5 TEOT: 7 TPAOH:1200 H_2O) is not conducive to film formation. The strong alkaline mixture was observed to etch and dissolve the silicon substrate. A considerable amount of effort was spent on identifying the optimum range of synthesis composition and conditions for the deposition of TS-1 zeolites in microchannels in terms of titanium incorporation, crystal size, and crystal intergrowth (40 TEOS:0–1.6 TEOT: 10–14 TPAOH:0–0.4 TEMS:10,000 H_2O; 448 K).

It has been suggested that the isolated, tetrahedral Ti(IV) ions in the –Si–O–Ti–O–Si– zeolite matrix are the active sites for the reaction while octahedrally coordinated Ti(IV) is inactive [40]. The mechanism of 1-pentene epoxidation involves the formation of active titanium (IV) hydroperoxide intermediates by hydrogen peroxide solvolysis [41]. During the reaction the oxygen atom located next to the metal center initiates the reaction by attacking the carbon–carbon double bond of alkene molecules [42]. Early efforts led to poor titanium insertion in the zeolite framework as indicated by the XPS data shown in Figs. 2a and 2b. Titanium (IV) ions located at the tetrahedral position of the silicalite framework have Ti $2p_{3/2}$ and Ti $2p_{1/2}$ binding energies of 460 and 466 eV, respectively [43–45]. The octahedrally coordinated Ti(IV) attributed to extraframework titanium atoms have a Ti $2p_{3/2}$ binding energy of 458 eV and Ti $2p_{1/2}$ of 464 eV [43–45].

Fig. 2a represents a sample prepared by a TS-1 synthesis mixture with a Si/Ti ratio of 1 (40 TEOS:40 TEOT:10 TPAOH:10,000 H_2O). Very little titanium is present in the sample and this may be due to the incomplete hydrolysis of TEOT. Catalysts prepared by this solution were inactive for epoxidation. Using a synthesis composition with a higher ratio of Si/Ti (e.g., 40 TEOS:1.6 TEOT:0.4 TEMS: 14 TPAOH:10,000 H_2O), better titanium incorporation was observed (Fig. 2b). However, only a portion of the total titanium ($\sim 48\%$) was present in the zeolite framework. There was considerable amount of extraframework titanium in these samples. Although they were active for epoxidation, the results showed poor reproducibility since the amount of framework titanium varied significantly even for samples made from the same synthesis procedure. The problem was attributed to presence of alkali impurities in the TEOS reagent.

The presence of alkali has been reported to inhibit titanium substitution in TS-1 zeolite [46]. Near complete (i.e., $> 80\%$) insertion of titanium in zeolite framework was obtained from the same synthesis solution composition as in Fig. 2b after ensuring that the TEOS reagent was free of most alkali impurities (Fig. 2c). Extra care must be taken to ensure that all apparatuses were completely dry to prevent the hydrolysis of titanium compounds into hydrated TiO_2. These simple precautions enabled us to reproducibly prepare TS-1 zeolite microreactors with a titanium content of up to 3.5 at.%. Five microreactors were prepared and coated with TS-1 zeolite film to test the reproducibility. The TS-1 was grown from a synthesis solution containing 40 TEOS: 1.6 TEOT:0.4 TEMS:14 TPAOH:10,000 H_2O, at 448 K, for 24 h. Analyses showed that the deposited zeolite catalysts

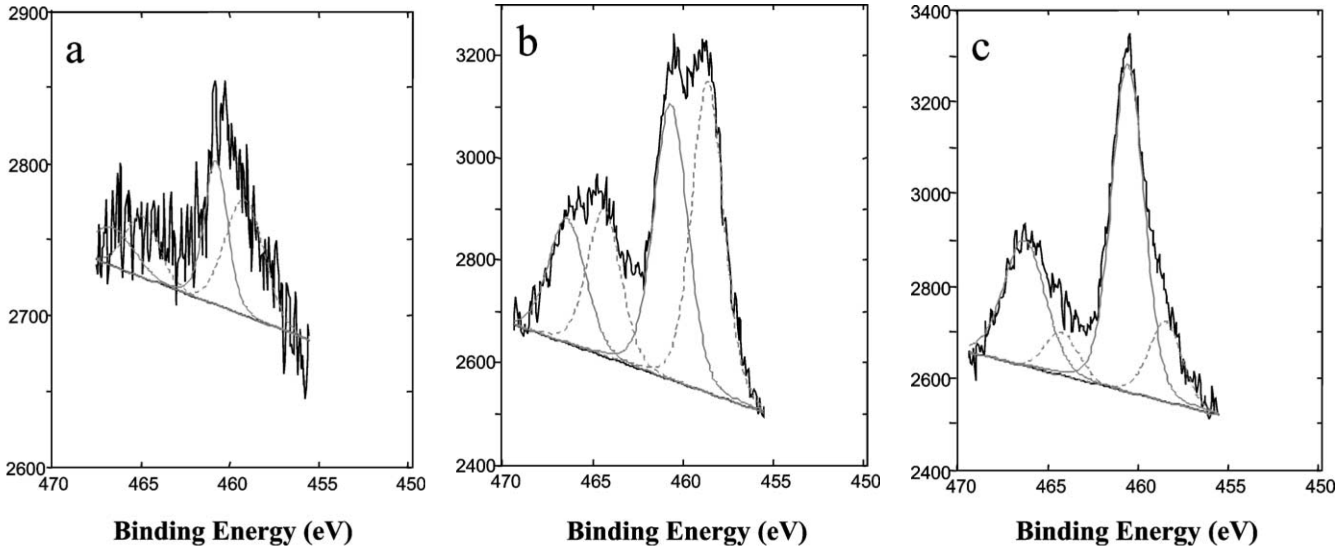

Fig. 2. X-ray photoelectron spectra of (a, b) partial and (c) near complete insertion of titanium into the TS-1 zeolite framework. (Note: solid lines correspond to the tetrahedrally coordinated framework Ti(IV) and broken lines refer to the octahedrally coordinated extraframework Ti(IV).)

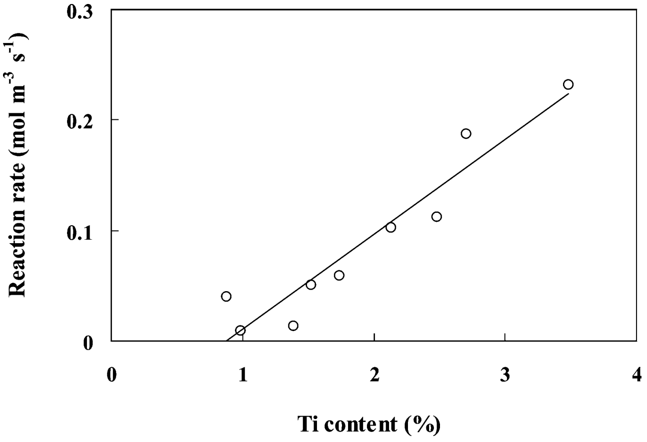

Fig. 3. Initial epoxypentane production rate as a function of framework titanium content of TS-1 zeolite microreactors.

had a titanium content of 1.7–2.4 at.%. They also displayed comparable film morphology with an average crystal size and film thickness of 2.2 and 5 µm, respectively. Reaction tests on the microreactors showed reproducible results. An epoxypentane yield of 5.5 ± 0.5% was measured. The yield was defined as the ratio of the amount of 1,2-epoxypentane produced to the initial amount of hydrogen peroxide, which is the limiting reagent. 1,2-Epoxypentane was the main product with only traces of glycol monoethylether.

The effects of TS-1 framework titanium content on the reaction were investigated for a fixed catalyst amount (i.e., 5-µm-thick TS-1 film or 8×10^{-5} g catalyst). Fig. 3 shows the initial epoxypentane production rate as a function of framework titanium content of TS-1 zeolite microreactors. The plot demonstrates that the catalysts with less than 1 wt% Ti were inactive for the reaction and the reaction rate increases in proportion to the titanium content of the TS-1 zeolite. The SEM pictures in Fig. 4 show the microstructure of three TS-1 zeolite microreactors used in Fig. 3. The framework titanium contents of the TS-1 zeolites shown in Figs. 4a, 4b, and 4c are 1.6, 2.0, and 2.5 at.%, respectively. The TS-1 grown on the uniformly seeded microchannel forms an intergrown zeolite film with a preferred (101) orientation. The zeolite film evenly coats the surface of the 500-µm-wide microreactor channel. Films of comparable crystal size, intergrowth, and thickness were obtained by careful manipulation of the synthesis composition. All three catalyst films display similar film morphology and crystal intergrowth with average crystal size of 2.2 ± 0.2 µm and thickness of 5 ± 0.1 µm (Fig. 4), similar to all samples used for the experiments in Fig. 3.

3.3. *Effect of film orientation and crystal size*

In previous publications [16,47], the influence of seed concentration on the morphology and orientation of deposited zeolite film was described. Figs. 5a and 5b display the microstructures of two TS-1 films grown from the same synthesis solution on clean and seeded microchannels. On

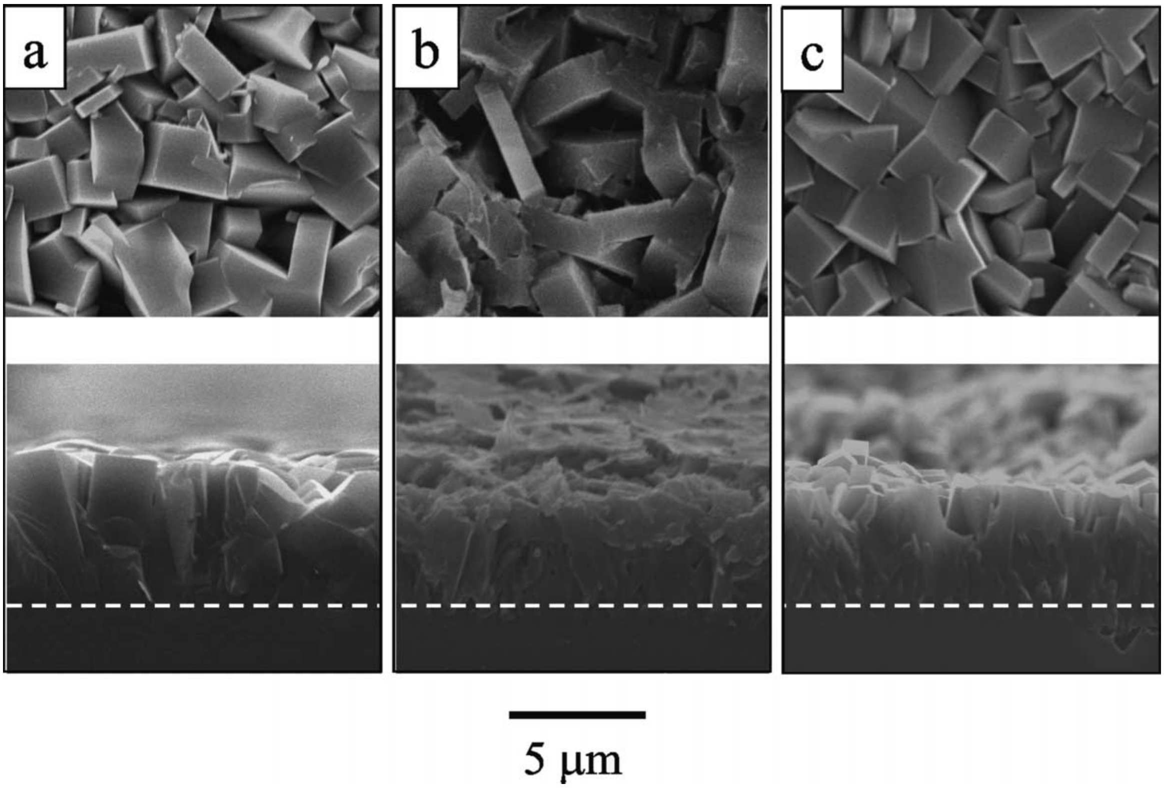

Fig. 4. Scanning electron microscope pictures of TS-1 zeolite microreactors with a framework titanium content of (a) 1.6, (b) 2.0, and (c) 2.5 at.%. (Note: the top view pictures are twice the magnification of the cross section.)

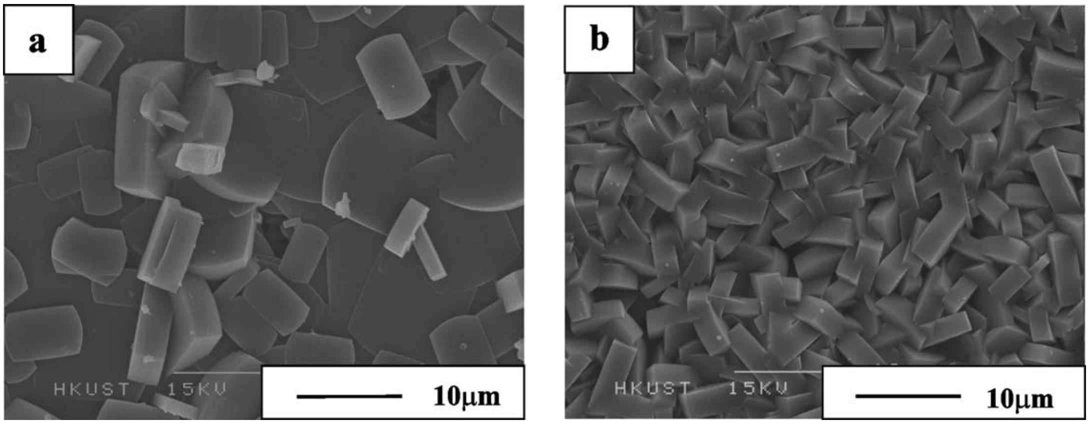

Fig. 5. Scanning electron microscope pictures of TS-1 zeolite grown on (a) unseeded and (b) seeded silicon microchannels. The films were regrown from a synthesis solution containing 40 TEOS:1.6 TEOT:10 TPAOH:10,000 H_2O at 448 K for 24 h.

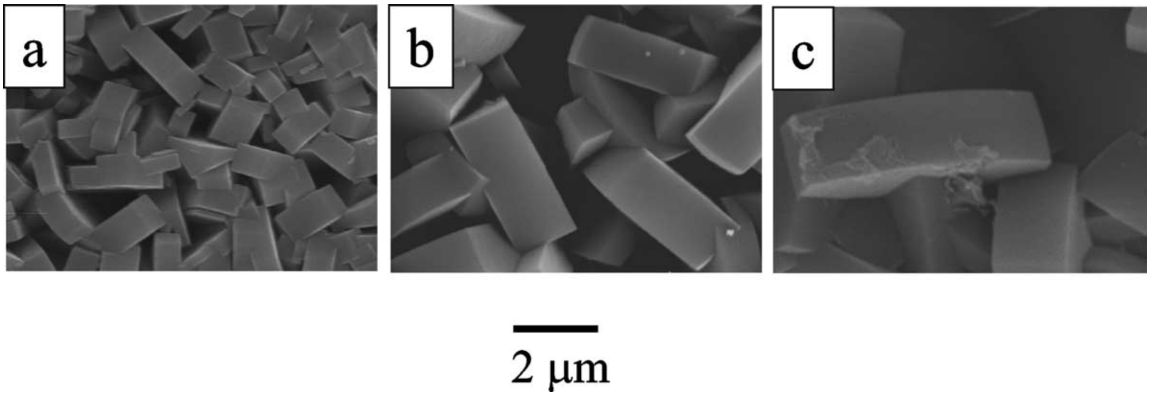

Fig. 6. Scanning electron microscope pictures of TS-1 zeolite microreactors with average crystal sizes of (a) 2 (40 TEOS:1.6 TEOT:0.4 TEMS: 14 TPAOH:10,000 H_2O), (b) 3 (40 TEOS:1.6 TEOT:14 TPAOH:10,000 H_2O), and (c) 4 μm (40 TEOS:1.6 TEOT:10 TPAOH:10,000 H_2O).

the unseeded substrate (Fig. 5a) the prismatic, TS-1 zeolites were deposited with their (020) crystal plane parallel to the channel floor. This means that the straight MFI zeolite pore channels were aligned normal to the substrate, while the zigzag channels ran parallel to the channel surface. Secondary growth is evident from the presence of multilayered deposits that consisted of smaller zeolite crystals. The secondary crystals grew with their (200) planes parallel to the first layer of (020) zeolite film as shown in the figure. X-ray diffraction analysis confirmed that the film possessed a (200/020) preferred orientation. The microchannel was covered with approximately 3.8×10^{10} zeolite crystals/m^2 with an average size of 6 × 8 μm. Neighboring crystals merged to form an intergrown layer that was occasionally interrupted by defects caused by mismatched growth.

TS-1 zeolites grown on seeded microchannels from the same synthesis solution and regrowth conditions display a different morphology and crystal habit as shown in Fig. 5b. An inverted pyramidal shape evolved as the zeolite grew from the individual seeds. The seed resided at the apex of the pyramidal zeolite grain that terminated on a (101)-crystallographic plane. The XRD pattern displayed predominantly the (101) diffraction line. In this orientation, molecules must diffuse through the zeolite by hopping between the intersecting straight and zigzag zeolite pore channels. The film consisted of 5.5×10^{11} zeolite crystals/m^2 with an average grain size of 2 × 4 μm. The anisotropic growth behavior of TS-1 and the crystal habit of the deposited zeolites are responsible for the observed difference in the film morphology, crystal size, and film thickness of TS-1(200/020) and TS-1(101) [16].

The microreactor coated with TS-1(020/200) film displayed low activity for 1-pentene epoxidation. The overall reaction rate was 9×10^{-4} mol/(m^3 s), despite having more accessible pore channels (i.e., straight pores). Because of the increased surface roughness and smaller crystal size, the (101) zeolite-coated microreactors exhibited a higher reaction rate (6.3×10^{-3} mol/(m^3 s), even though the reacting molecules are expected to hop between straight and zigzag pore channels. The observed behavior is attributed to the larger contact area between reactants and catalyst for TS-1 (101) versus TS-1(020/200) (i.e., 37.4 versus 4.0 m^2/m^2).

The effect of crystal size was investigated by adding triethoxymethylsilane in the synthesis solution which acts as crystal growth inhibitor and employing alternate growth conditions. Fig. 6 displays SEM images of TS-1(101) films with average crystal sizes of 2, 3, and 4 μm. Although the TS-1 films shown in Fig. 6 have different crystal sizes, they

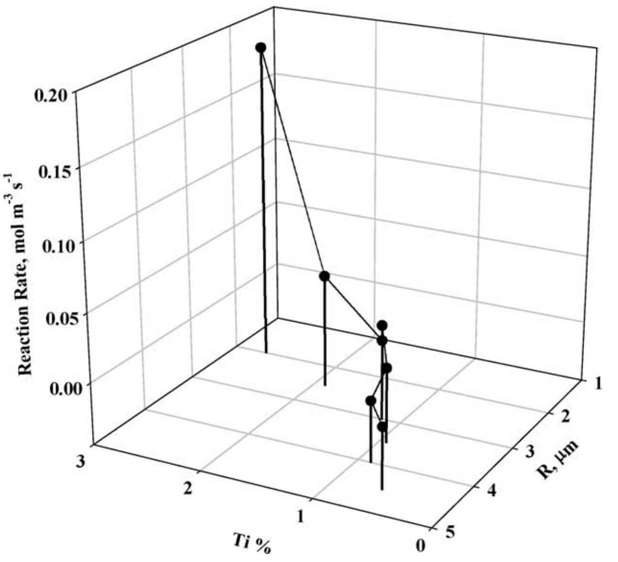

Fig. 7. Initial epoxypentane production rate as a function of crystal size and framework titanium content.

possess similar surface morphology and film thickness (i.e., 5 ± 0.5 μm). The Ti content is 0.9–2.7 at.%. The smallest crystal size was obtained by adding TEMS and adjusting the OH^-/Si^- ratio to 0.35 (Fig. 6a). Larger crystals were grown from solution without TEMS and a lower OH^-/Si^- (Figs. 6b and 6c). Fig. 7 shows the initial overall reaction rate as a function of crystal size and titanium content. In addition to the fact that reaction rate is higher for high Ti loadings, the figure shows that reaction rate is higher for TS-1 films with smaller crystal size and hence larger external surface area available for reaction. This indicates that intracrystalline diffusional resistances are significant.

3.4. Catalyst deactivation

A series of experiments were conducted to investigate the deactivation of TS-1 catalyst in the microreactor. The reaction was interrupted and quenched at regular time intervals of 5 h. The TS-1 zeolite microreactor was disassembled, cleaned, and dried before it was regenerated by air calcination at 823 K and analyzed by XPS. Two deactivation processes were identified: a short-term reversible deactivation over a period of few hours, and an overall long-term, irreversible deactivation (Fig. 8). It was suspected that the short-term deactivation was due to the presence of organic compounds blocking the active sites and pores of TS-1.

To further understand catalyst deactivation, TGA/DTA experiments were carried out on TS-1 powder prepared from the same synthesis conditions as the TS-1 zeolite microreactor. One hundred milligrams of the powder catalyst was used for epoxidation in a batch reactor (i.e., 0.9 M 1-pentene and 0.2 M H_2O_2 for 50 h at 50 ml reaction mixture). The catalyst was dried in an oven at 333 K before the TGA experiment. The sample was heated in air from room temperature to 1073 K at a heating rate of 5 K/min. A total of 38% loss in mass was measured for the whole experiment, 35% of which occurred at a temperature of 373 K and coincided with an endothermic heat flow of 640 J/g that is comparable to the heat of evaporation of adsorbed water. The remaining 3% mass loss was attributed to desorption and decomposition of adsorbed organic compounds. It seems that water and organic by-products play a significant role in TS-1 catalyst deactivation.

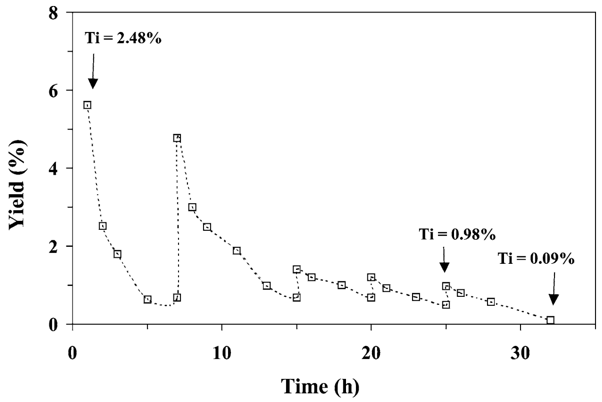

Fig. 8. 1,2-Epoxypentane yield as a function of time on stream. Catalyst regeneration was carried out at 7, 15, 20, and 25 h and the titanium loading was determined by XPS at 1, 25, and 32 h.

In propylene epoxidation, TS-1 deactivates when propylene oxide oligomers deposit inside the zeolite pores. The catalyst is regenerated when the oligomers are removed by either calcination in air at 773 K [38] or reflux in dilute hydrogen peroxide [48]. Uguina et al. [49] have studied the deactivation of TS-1 during styrene oxidation with hydrogen peroxide and observed a decline in the catalyst reactivity with time. The presence of diffusional limitations arising from a high degree of occupancy of the TS-1 pores and strong adsorption of styrene, phenylacetaldehyde, and benzaldehyde on the Ti sites were proposed as the main reasons for deactivation. Thiele and Roland [48] further argue that the coordination of water to the active site increases the acidity and hence the propensity for by-product formation. A similar deactivation process may be present in this work as suggested by the TGA/DTA results.

The long-term, irreversible deactivation of TS-1 can be attributed to leaching of framework titanium atoms [38,51]. XPS analysis showed that the amounts of tetrahedrally coordinated titanium present in the catalyst at 1, 25, 32 h were 2.48, 0.98, and 0.09 at.%, respectively (Fig. 8). XPS studies showed that another TS-1 microreactor with an initial framework titanium loading of 1.1 at.% lost about 30% of the titanium after immersing in the reaction solution (ca. 50 ml) at room temperature for 5 h. A further 25% loss in framework titanium (from 0.8 to 0.6 at.%) was observed after the regeneration treatment at high temperatures. To identify the cause of titanium leaching, a set of experiments was conducted using TS-1 zeolite powder with a framework titanium content of 0.6 at.%. A 0.1 g of TS-1 zeolite was immersed in a solution containing 0.2 M H_2O_2 and 0.7 M H_2O in methanol at room temperature for 5 h with constant stirring. After drying, analysis with XPS revealed that the framework titanium content had decreased to 0.5 at.%. A larger decrease in titanium content (0.6 to 0.2 at.%) was observed when TS-1 was immersed in a solution with higher water concentration (i.e., 0.2 M H_2O_2, 1.5 M H_2O in methanol).

The above results are consistent with the assertion that leaching occurs through solvolysis by polar molecules such as water and hydrogen peroxide that react with the tetrahedral titanium to form octahedral titanium peroxo species [38]. Titanium removed from TS-1 during reaction may also originate from defect sites in the framework where Ti is not perfectly coordinated to the four O–Si groups [51,52]. Such defect sites have been proposed by Lamberti et al. [53] who observed that TS-1 can be highly defective. There is a possibility that TS-1 prepared using a short crystallization period may have an increased concentration of these defect sites [51]. Furthermore, it has been observed that titanium leaching is more prevalent under continuous flow conditions [52]. It is possible that the equilibrium established between the solution Ti species and the Ti on the catalyst surface is perturbed under such conditions.

4. Concluding remarks

Titanium silicalite-1 films were grown within the channels of microstructured silicon reactors. The deposited TS-1 films were active for catalyzing 1-pentene epoxidation to produce 1,2-epoxypentane. Preparation conditions which give a high framework titanium content and small crystal size produced catalysts with higher reaction rates, the latter indicating the presence of mass-transfer resistances. Irreversible deactivation was observed during the course of the experiments and was attributed to leaching of framework titanium by water and hydrogen peroxide. Short-term reversible deactivation was due possibly to deposited organic compounds.

Acknowledgment

We thank the UK's Engineering and Physical Sciences Research Council (EPSRC), the Hong Kong Research Grant Council (HKUST6021/01P and HKUST6009/02P), and the Institute for Integrated Microsystems (I2MS-01/02.EG02) for funding this research. Y.S.S. Wan thanks the Croucher Foundation for her scholarship.

References

[1] E.V. Rebrov, G.B.F. Seijger, H.P.A. Calis, M.H.J.M. de Croon, C.M. van den Bleek, J.C. Schouten, Appl. Catal. A. 206 (2001) 125.

[2] Y.S.S. Wan, A. Gavriilidis, J.L.H. Chau, K.L. Yeung, Chem. Commun. 8 (2002) 878.

[3] S.M. Lai, R. Martin-Aranda, K.L. Yeung, Chem. Commun. 2 (2003) 218.

[4] J.L.H. Chau, A.Y.L. Leung, M.B. Shing, K.L. Yeung, C.M. Chan, in: Z. Tang, P. Sheng (Eds.), Nano Science and Technology: Novel Structure and Phenomena, Taylor & Francis, London, 2003.

[5] J.L.H. Chau, A.Y.L. Leung, K.L. Yeung, in: Design, Fabrication and Performance of Zeolite Micromembranes, ISCRE-17, Hong Kong, August 25–28, 2002.

[6] J.K. Robertson, Sens. Actuators A: Phys. 91 (2001) 333.

[7] J.M. Thomas, W.J. Thomas, Principles and Practice of Heterogeneous Catalysis, VCH, New York, 1997.

[8] A. Kursawe, D. Hönicke, Proceedings of the 4th Inter. Conf. on Microreaction Technol., Atlanta, 2000, pp. 153–166.

[9] G. Wießmeier, D. Hönicke, Ind. Eng. Chem. Res. 35 (1996) 4412.

[10] G. Wießmeier, D. Hönicke, J. Micromech. Microeng. 6 (1996) 285.

[11] S.K. Ajmera, M.W. Losey, K.F. Jensen, M.A. Schmidt, AIChE J. 47 (2001) 1639.

[12] J.C. Jansen, G.M. van Rosmalen, J. Crystals Growth 128 (1993) 1150.

[13] B.J. Schoeman, A. Erdem-Senatalar, J. Hedlund, J. Sterte, Zeolites 19 (1997) 21.

[14] M.J. den Exter, H. van Bekkum, C.J.M. Rijn, F. Kapteijn, J.A. Moulijn, H. Schellevis, C.I.N. Beenakker, Zeolites 19 (1997) 13.

[15] J. Hedlund, S. Mintova, J. Sterte, Micropor. Mesopor. Mater. 28 (1999) 185.

[16] S.M. Lai, L.T.Y. Au, K.L. Yeung, Micropor. Mesopor. Mater. 54 (2002) 63.

[17] Y.S.S. Wan, J.L.H. Chau, A. Gavriilidis, K.L. Yeung, Micropor. Mesopor. Mater. 42 (2001) 157.

[18] J.L.H. Chau, K.L. Yeung, Chem. Commun. 9 (2002) 960.

[19] J.L.H. Chau, A.Y.L. Leung, K.L. Yeung, Lab-on-a-Chip. 3 (2003) 53.

[20] B. Notari, Adv. Catal. 41 (1996) 253.

[21] M.G. Clerici, Appl. Catal. 68 (1991) 249.

[22] M.G. Clerici, Stud. Surf. Sci. Catal. 78 (1993) 21.

[23] M.G. Clerici, P. Ingallina, J. Catal. 140 (1993) 71.

[24] G. Langhendries, D.E. De Vos, G.V. Baron, P.A. Jacobs, J. Catal. 187 (1999) 453.

[25] I. Schmidt, A. Krogh, K. Wienberg, A. Carlsson, M. Brorson, C.J.H. Jacobsen, Chem. Commun. (2000) 2157.

[26] F. Maspero, U. Romano, J. Catal. 146 (1994) 476.

[27] P. Ingallina, M.G. Clerici, L. Rossi, G. Bellussi, Stud. Surf. Sci. Catal. 92 (1995) 31.

[28] T. Atoguchi, S. Yao, J. Mol. Catal. A: Chem. 176 (2001) 173.

[29] S. Gontier, A. Tuel, Appl. Catal. A 118 (1994) 173.

[30] W.R. Sanderson, Pure. Appl. Chem. 72 (2000) 1289.

[31] R.A. Sheldon, Chemtech 24 (1994) 38.

[32] R.A. Sheldon, J. Chem. Technol. Biotechnol. 68 (1997) 381.

[33] C. Perego, A. Carati, P. Ingallina, M.A. Mantegazza, G. Bellussi, Appl. Catal. A 221 (2001) 63.

[34] L. Dal Pozzo, G. Fornasari, T. Monti, Catal. Commun. 3 (2002) 369.

[35] H. Gao, G. Lu, J. Suo, S. Li, Appl. Catal. A 138 (1996) 27.

[36] G.J. Hutchings, D.F. Lee, A.R. Minihan, Catal. Lett. 33 (1995) 369.

[37] S.B. Kumar, S.P. Mirajkar, G.C.G. Pais, P. Kumar, R. Kumar, J. Catal. 156 (1995) 163.

[38] L.Y. Chen, G.K. Chuah, S. Jaenicke, J. Mol. Catal. A 132 (1998) 281.

[39] A. Carati, C. Flego, D. Berti, R. Millini, C. Perego, B. Stocchi, C. Perego, Stud. Surf. Sci. Catal. 125 (1999) 45.

[40] E. Duprey, P. Beaunier, M.A. Springuel-Huet, F. Bozon-Verduraz, J. Fraissard, J.M. Manoli, J.M. Brégeault, J. Catal. 165 (1997) 22.

[41] R.S. Drago, S.C. Dias, J.M. McGilvray, A.L.M.L. Mateus, J. Phys. Chem. B 102 (1998) 1508.

[42] D. Tantanak, M.A. Vincent, I.H. Hillier, Chem. Commun. (1998) 1031.

[43] S.M. Mukhopadhyay, S.H. Garofalini, J. Non-Cryst. Solids 126 (1990) 202.

[44] D.T. On, L. Bonnevoit, A. Bittar, A. Sayari, S. Kaliaguine, J. Mol. Catal. 74 (1992) 233.

[45] G.N. Vayssilov, Catal. Rev.-Sci. Eng. 39 (1997) 209.

[46] G. Perego, R. Millini, G. Bellussi, in: H.G. Karge, J. Weitkamp (Eds.), Molecular Sieves: Science and technology, vol. 1, Springer, Berlin, 1998, p. 187.

[47] J.L.H. Chau, Y.S.S. Wan, A. Gavriilidis, K.L. Yeung, Chem. Eng. J. 88 (2002) 187.

[48] G.F. Thiele, E. Roland, J. Mol. Catal. A 117 (1997) 351.

[49] M.A. Uguina, D.P. Serrano, R. Sanz, J.L.G. Fierro, M. López-Granados, R. Mariscal, Catal Today 61 (2000) 263.

[50] R.A. Sheldon, M. Wallau, I.W.C.E. Arends, U. Schuchardt, Acc. Chem. Res. 31 (1998) 485.

[51] L. Davies, P. McMorn, D. Bethell, P.C.B. Page, F. King, F.E. Hancock, G.J. Hutchings, Phys. Chem. Chem. Phys. 3 (2001) 632.

[52] L. Davies, P. McMorn, D. Bethell, P.C.B. Page, F. King, F.E. Hancock, G.J. Hutchings, J. Catal. 198 (2001) 319.

[53] C. Lamberti, S. Bordiga, D. Arduino, A. Zecchina, F. Geobaldo, G. Spano, F. Genoni, G. Petrini, A. Carati, F. Villain, G. Vlaic, J. Phys. Chem. B 102 (1998) 6382.